Electrocatalysis (2015) 6:173–178
DOI 10.1007/s12678-014-0231-0

On the Temperature Performance of Ethanol Oxidation Reaction at Palladium-Activated Nickel Foam

Boguslaw Pierozynski · Tomasz Mikolajczyk · Marcin Turemko

Published online: 1 October 2014

Abstract The present paper reports on ethanol oxidation reaction (EOR) investigated at catalytically modified nickel foam material. The EOR was studied in 0.1 M NaOH supporting electrolyte on Pd-activated nickel foam catalyst material, obtained by a spontaneous deposition method. Catalytic modification of Ni foam resulted in a composite material having superior EOR kinetics, as elucidated through corresponding values of a.c. impedance-derived charge-transfer resistance parameter (including temperature-dependence of the EOR over the temperature range 20–60 °C). The presence of a catalytic additive was disclosed from SEM and XRD analyses.

Keywords Nickel foam · Ethanol oxidation reaction · Pd activation · Electrochemical impedance spectroscopy

Introduction

Electrooxidation of ethanol attracts significant attention because of its potential application in direct ethanol fuel cells (DEFCs) [1]. Ethanol is an important renewable fuel, which could conveniently be produced in great quantities, e.g. by fermentation of sugar-containing biomass. As compared to methanol, its key competitor, ethanol is not only characterized by significantly higher (by *ca*. 30 %) energy density but is also substantially non-toxic [2, 3]. The most desired anodic reaction for a DEFC device is complete oxidation of a C_2H_5OH molecule to form water and CO_2. However, ethanol oxidation reaction (EOR) typically leads to numerous intermediates and by-products that could potentially become adsorbed on the catalyst surface. In fact, the main difficulty here (especially at low-operating temperatures) is to achieve significant cleavage of the C–C bond [2].

As kinetics of ethanol oxidation process were found to become significantly facilitated in alkaline environments [4–8], the range of suitable EOR catalyst materials was extended to cover non-noble but highly corrosion-resistant metals, such as nickel, which also possesses reasonable electrical and thermal conductivities and good mechanical durability [9, 10]. Nickel foams have commercially been available for more than two decades. Application of highly modifiable base material having large specific surface area is of superior importance for the development of low noble metal level, highly electroactive catalyst composites. In this respect, nickel foam might potentially become a key player within such important electrochemical technologies as alkaline PEM fuel cells, water electrolysers, hydrogen storage and pollutant degradation systems [11–13].

In this study, Pd-modified Ni foam sample electrodes were prepared by means of a spontaneous deposition method, as described in ref. 13. Such obtained catalyst materials were employed as electrocatalysts for the EOR over the temperature range 20–60 °C, in 0.1 M NaOH supporting electrolyte. Palladium was chosen, as Pd was previously found to exhibit high catalytic activity for ethanol oxidation in alkaline media, along with superior tolerance against CO poisoning effect [14–18]. It should be stressed that pure Ni foam itself does not possess any electrocatalytic activity towards the EOR [19]. However, nickel foam material could be made catalytic for alcohol oxidation reaction through the surface formation of extensive oxide/hydroxide layer [20].

B. Pierozynski (✉) · T. Mikolajczyk · M. Turemko
Department of Chemistry, Faculty of Environmental Management and Agriculture, University of Warmia and Mazury in Olsztyn, Plac Lodzki 4, 10-957 Olsztyn, Poland
e-mail: bogpierozynski@yahoo.ca

B. Pierozynski
e-mail: boguslaw.pierozynski@uwm.edu.pl

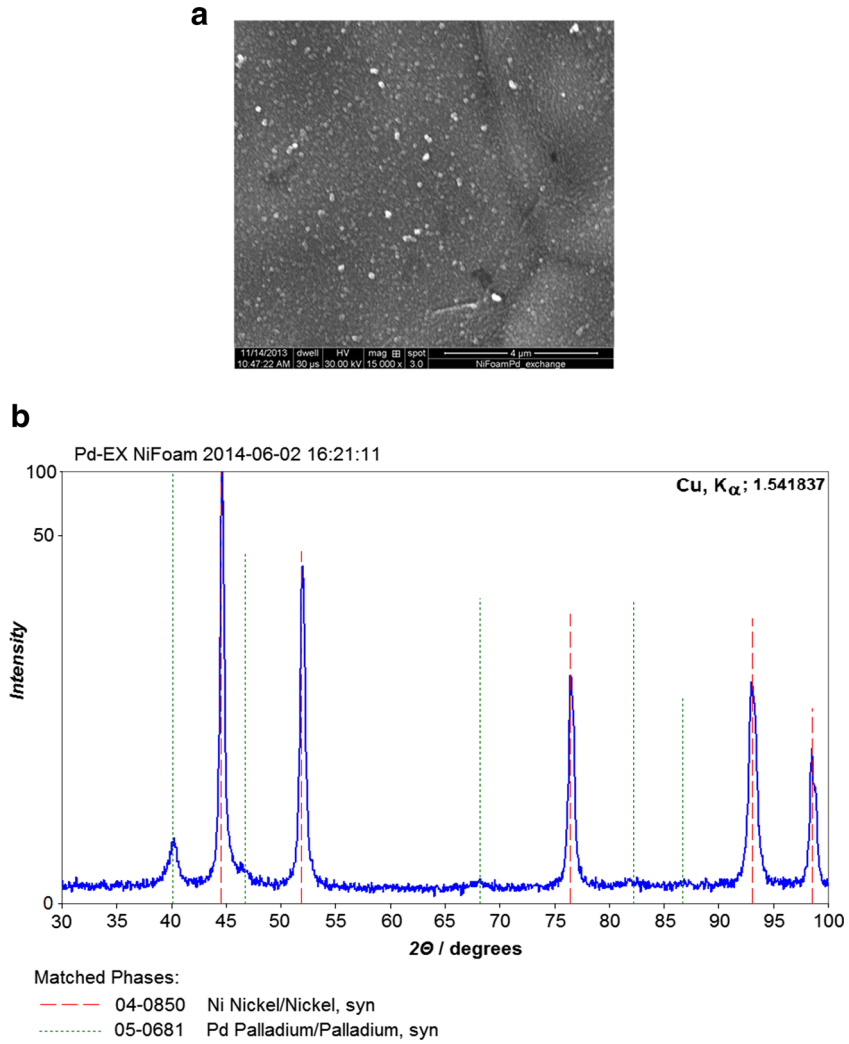

Fig. 1 **a** SEM micrograph picture of Pd-modified Ni foam surface (*ca.* 0.27 wt% Pd), taken at 15,000× magnification; **b** XRD pattern for spontaneously deposited Pd element on Ni foam substrate; diffraction lines correspond to the following sequence of fcc indices: (111), (200), (220), (311) and (222) for both Ni and Pd elements

Experimental

An electrochemical cell made of Pyrex glass was used during the course of this work. The cell comprised three electrodes: a Ni foam-based working electrode (WE) in a central part, a reversible Pd (0.5 mm diameter, 99.9 % purity, Aldrich) hydrogen electrode (RHE) as reference and a Pt (1.0 mm diameter, 99.9998 % purity, Johnson Matthey, Inc.) counter electrode (CE), both placed in separate compartments. Nickel foam was provided by MTI Corporation (purity: >99.99 % Ni; thickness: 1.6 mm; surface density: 346 g m^{-2}; porosity: ≥95 %), where no information on the specific surface area of this foam was given. However, the electrochemically active surface area of the MTI foam has been estimated at 19.2 cm^2 (548 cm^2 g^{-1}) in recent work from this laboratory [21] (compare with similar values recorded by Grden et al. [22] and by van Drunen et al. [23], based on the impedance and the cyclic voltammetry-derived data, correspondingly). All studied working electrodes were 1 cm×1 cm. Spontaneous deposition of Pd on nickel foam samples [13] was carried out in several steps: Freshly cut foam samples were subjected to acetone and CH_2Cl_2 wash (15 min+ultrasonication), following air drying and acid etching in 2 M HCl (15 min at 60 °C); then,

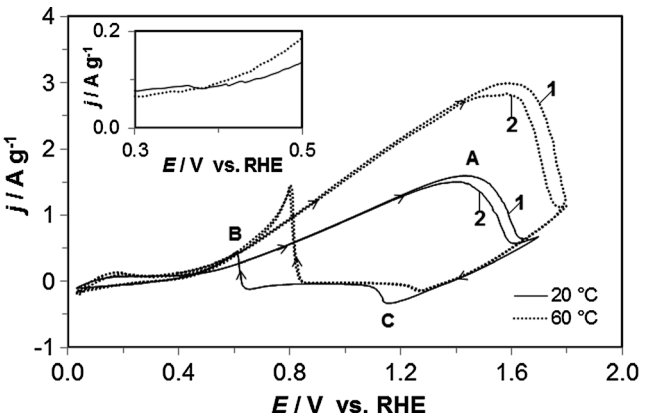

Fig. 2 Cyclic voltammograms for ethanol electrooxidation on Pd-modified Ni foam, carried out in 0.1 M NaOH, at a sweep rate of 50 mV s^{-1} and in the presence of 0.25 M C_2H_5OH, at the stated temperature values (notations 1 and 2 correspond to the sequence of sweeps)

Table 1 Resistance and capacitance parameters for electrooxidation of ethanol (at 0.25 M C_2H_5OH) on Pd-modified Ni foam electrode in 0.1 M NaOH, obtained by finding the equivalent circuit, which best fitted the impedance data, as shown in Fig. 4

E/mV	20 °C	30 °C	40 °C	50 °C	60 °C
R_{ct}/Ω g					
400	3.04±0.11	3.35±0.10	2.40±0.05	1.70±0.03	1.70±0.03
500	1.06±0.02	0.89±0.01	0.68±0.01	0.47±0.00	0.42±0.00
600	0.38±0.00	0.34±0.00	0.26±0.00	0.20±0.00	0.18±0.00
700	0.24±0.00	0.20±0.00	0.16±0.00	0.12±0.00	0.12±0.00
800	0.21±0.00	0.15±0.00	0.13±0.00	0.11±0.00	0.09±0.00
900	0.17±0.00	0.13±0.00	0.11±0.00	0.09±0.00	0.09±0.00
1,000	0.14±0.01	0.12±0.00	0.10±0.00	0.08±0.00	0.08±0.00
1,100	0.17±0.00	0.12±0.00	0.11±0.00	0.09±0.00	0.09±0.00
1,200	0.24±0.00	0.14±0.00	0.15±0.00	0.12±0.00	0.11±0.00
1,400	0.45±0.02	0.16±0.01	0.17±0.00	0.17±0.00	0.16±0.00
C_{dl}/μF g^{-1} $s^{\varphi 1-1}$					
400	263,713±4,243	183,375±2,745	158,161±2,052	127,131±1,969	106,349±1,871
500	162,442±3,122	128,724±2,313	106,410±1,958	86,818±1,851	76,523±1,482
600	134,705±3,397	117,509±2,637	96,381±2,779	80,579±2,630	76,622±3,103
700	134,611±4,268	119,327±3,110	100,592±4,540	86,105±4,205	78,373±4,873
800	150,710±5,258	120,453±4,130	120,314±7,282	141,405±10,478	85,930±4,933
900	159,255±6,822	134,115±6,483	143,048±9,728	124,853±10,468	174,619±13,592
1,000	147,172±12,416	144,997±6,732	159,166±9,476	138,914±7,447	167,777±9,524
1,100	194,201±6,670	199,212±12,752	238,129±13,213	206,190±8,604	205,826±13,105
1,200	304,182±8,633	259,464±11,716	420,214±18,831	339,678±16,535	293,914±19,801
1,400	2,684,182±62,974	433,110±32,912	890,214±24,715	1,471,046±40,855	1,482,735±43,741

spontaneous deposition of Pd was realized by dipping such pretreated foam electrodes in 0.005 M $PdCl_2$ (pH=1.0, $t_{dep.}$= 30 s and $T_{dep.}$=25±1 °C) to obtain Pd-modified Ni foam composite electrodes. Cyclic voltammetry and electrochemical impedance spectroscopy techniques were employed in this work. All measurements were registered over the temperature range 20–60 °C by means of *Solatron* 12,608 W Full Electrochemical System. Data analysis was performed with *ZView 2.9* (*Corrview 2.9*) software package, where the impedance spectra were fitted using a complex, non-linear, least-squares immitance fitting program *LEVM 6*, written by J.R. Macdonald [24]. All other experimental details, including preparation of supporting electrolyte (0.25 M C_2H_5OH in 0.1 M NaOH), pretreatments applied to electrochemical cell and electrodes, and employed a.c. impedance protocol were as those given in refs. 7, 8 and 18.

Results and Discussion

A sample of Pd-modified (at. *ca*. 0.27 wt% Pd) MTI-delivered Ni foam material, recorded for the magnification of 15,000× is shown in a SEM micrograph picture of Fig. 1a, where high density of homogeneously distributed small Pd nuclei could clearly be observed. In addition, the powder XRD-calculated (Siemens D500 powder diffractometer with CuK_α radiation; λ=1.5418 Å, *U*=38 kV, *I*=30 mA was used) average Pd grain size value came to 10.0±0.8 nm (see Fig. 1b). The above was accomplished by means of the Scherrer's method through correlation of the size of crystallite domains with relative

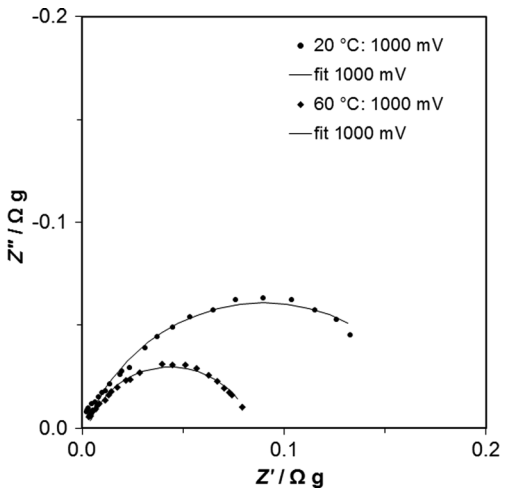

Fig. 3 Complex plane impedance plots for Pd-modified Ni foam in contact with 0.1 M NaOH, in the presence of 0.25 M C_2H_5OH, recorded at 1,000 mV at the stated temperature values. The *solid line* corresponds to representation of the data according to the equivalent circuit shown in Fig. 4

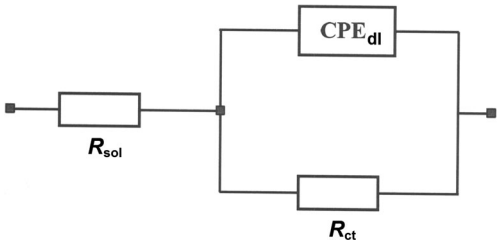

Fig. 4 Equivalent circuit used for fitting the obtained a.c. impedance spectroscopy data, where R_{sol} is solution resistance, CPE_{dl} is double-layer capacitance (represented as constant phase element to account for distributed capacitance) and R_{ct} is charge-transfer resistance parameter for electrooxidation of ethanol

widening of diffraction peaks [25]. Furthermore, SEM (Quanta FEG 250 scanning electron microscope was employed) grain size estimations were on the order of 10.0±1.0 nm.

Figure 2 below presents the cyclic voltammetric behaviour for the temperature-dependent process of ethanol electrooxidation (at 0.25 M C_2H_5OH), performed on Pd-modified Ni foam material in 0.1 M NaOH supporting solution. Hence, during the forward, 20 °C potential scan, a single oxidation peak A (centred at *ca*. 1.4 V vs RHE) appears in the voltammetric profile. However, upon the reverse scan towards the H_2 reversible potential, another oxidation peak (denoted as B and centred at about 0.6 V) emerges in the CV profile (see Fig. 2). While the latter, low potential peak, is usually assigned to oxidation of surface-adsorbed $CO_{ads.}$ species, the former peak corresponds to the formation of other EOR surface oxidation products but primarily to acetaldehyde [13, 26–29]. Furthermore, a small but discernible cathodic peak C, observable in the CV profile at *ca*. 1.1–1.3 V, most likely corresponds to the reduction of Ni(II) oxidation products [30], simultaneously formed during the EOR over the potential range 1.2–1.6 V RHE.

An increase of the reaction temperature from 20 to 60 °C caused significant amplification of the CV-recorded current densities. Interestingly, the corresponding centres for the high temperature peaks A and B became considerably shifted towards more positive potentials, both by *ca*. 200 mV (see Fig. 2 again). It should also be noted that the temperature increase has a significant impact on the EOR onset potential, which at 60 °C became substantially displaced towards the H_2 reversible potential (see inset to Fig. 2).

The reported here voltammetric EOR results are in good agreement with those recently reported for analogous experimental setup by Verlato et al. in ref. 13. However, for the former work, the voltammetric data format is presented here as per gram of the Ni foam/Pd composite (*ca*. 0.27 wt% Pd), whereas for the latter one, the CV results were displayed as per gram of pure Pd additive (see Fig. 11 in ref. 13). Thus, in order to make this comparison meaningful, one would have to multiply our current data presented in Fig. 2 by a factor of about 370×.

The a.c. impedance spectroscopy behaviour of the process of electrooxidation of ethanol (at 0.25 M C_2H_5OH) on the Pd-activated Ni foam electrode in 0.1 M NaOH is presented in Table 1 and Figs. 3 and 4 below. Hence, over the potential range 400–1,400 mV versus RHE, the impedance behaviour of the Pd-modified nickel foam is characterized by a single, partial and somewhat distorted semicircle, exhibited over intermediate and low frequencies in the Nyquist impedance spectra (see examples of impedance spectra obtained at two temperature extremes for the potential of 1,000 mV in Fig. 3). This semicircle corresponds to the charge-transfer resistance (R_{ct}) of the ethanol oxidation process. For 20 °C, the onset of ethanol oxidation could clearly be observed at about 400 mV in Fig. 2, which corresponds to 3.04 Ω g for the recorded R_{ct} parameter value. Then, over the potential range 400–1,400 mV, the charge-transfer resistance exhibited major reduction from 3.04 to 0.45 Ω g, respectively, where its minimum (0.14 Ω g) was recorded at 1,000 mV, prior to reaching the peak current potential value of the oxidation peak A. This

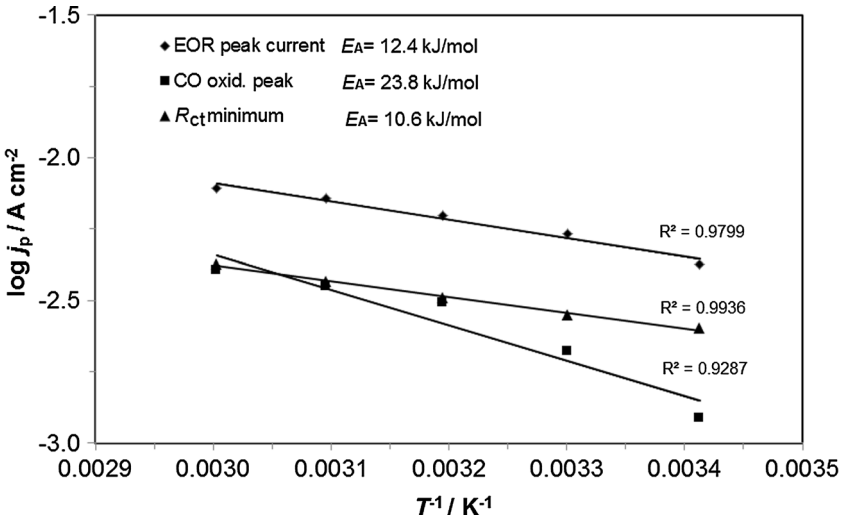

Fig. 5 Arrhenius plots for ethanol electrooxidation (at 0.25 M C_2H_5OH) on Pd-modified Ni foam electrode in contact with 0.1 M NaOH, recorded for the three stated potential values

behaviour most likely results from the fact that a major oxidation process is accompanied by a number of side reactions. Their intermediates become partly adsorbed on the catalyst's surface, thus inhibiting the kinetics of the key oxidation process. The above could be supported by dramatically increased double-layer capacitance, C_{dl} parameter, recorded at the potential values of 1,200 and 1,400 mV (Table 1), which does imply considerable contribution from surface adsorption processes that might take place over the corresponding potential range. Furthermore, the R_{ct} parameter revealed substantial temperature-dependent behaviour over the studied temperature range 20–60 °C, at all examined potential values. Thus, as an example, for the two extreme temperatures (20 and 60 °C), the R_{ct} parameter became reduced by *ca*. 1.8 and 2.9× for 400 and 1400 mV, respectively.

On the other hand, the double-layer capacitance (C_{dl}) parameter recorded for 20 °C for the potential range 400–1,100 mV exhibited some fluctuation (from 263,713 to 194,201 μF g^{-1} $s^{\phi 1-1}$, respectively). Taking into account a commonly used value of 20 μF cm^{-2} in literature as the C_{dl} value for smooth and homogeneous surfaces [31, 32] along with electrode mass of 37.3 mg, an electrochemically active surface area of the Pd-activated Ni foam could be estimated at *ca*. 492 cm^2 (at 400 mV) and 362 cm^2 at 1,100 mV RHE (which corresponds to 13,190 and 9,705 cm^2 g^{-1}, respectively). These values are dramatically higher than that reported for the unmodified Ni foam material in Experimental section above, as well as those recently recorded in works by Verlato et al. [13], Grden et al. [22] and by van Drunen et al. [23]. Similarly, a radical modification of electrochemically active surface area for nickel foam was achieved on Pt-modified (via chemically induced reduction) electrode in ref. [33], where this material was comprehensively evaluated with respect to its suitability for a number of electrochemical processes, including hydrogen/oxygen evolution and reduction reactions.

Interestingly, the C_{dl} parameter tends to become diminished upon temperature increase (most likely a consequence of increased surface blockage by intensified presence of reaction intermediates). On the other hand (as argued above), a dramatic increase of the C_{dl} for electrode potentials exceeding 1,100 mV most likely reflects pseudocapacitance components of the surface adsorption processes. Furthermore, in relation to the so-called *capacitance dispersion* effect [34, 35], the recorded values of a dimensionless parameter ϕ_1 (for the CPE component in Fig. 4) oscillated between 0.60 and 0.95.

In addition, the Arrhenius plot-derived (see Fig. 5) apparent activation energy (E_A) for electrooxidation of ethanol on the Pd-modified Ni foam catalyst material was derived for the three selected potentials, namely EOR peak current, CO oxidation peak current and minimum of the R_{ct} parameter. The recorded values of the E_A parameter came to 12.4, 23.8 and 10.6 kJ mol^{-1}, correspondingly. These are either in good agreement or else, they are significantly more favourable than those recently recorded for Pd/C [29] or Pd-bulk [14, 15] catalyst materials for the EOR, thus opening a serious opportunity for further development of large surface area, Pd-modified nickel foam anode materials, for commercial applications in direct ethanol fuel cells. These results may also be supported by work of Wang et al. [19], where a 3D-structured Ni foam/Pd electrode, fabricated by direct electrodeposition of palladium nanoparticles (10–40 and 100–150 nm), was shown (by cyclic voltammetry characterization) to exhibit significantly higher electroactivity in 1.0 M KOH than the corresponding Pd film electrode. The latter was (without getting into any detailed analysis) attributed to extensive modification of electrochemically active surface area for the Pd-modified Ni foam catalyst [19].

Conclusions

Large surface area, palladium-modified (at below 0.3 wt% Pd) nickel foam proved to possess highly catalytic properties towards electrooxidation of ethanol in 0.1 M NaOH supporting electrolyte. Reaction onset and the kinetics of EOR are strongly dependent on the reaction temperature. Also, recorded values of apparent activation energy for ethanol oxidation at Pd-modified Ni foam were either comparable or significantly more favourable than those derived under analogous conditions for Pd/C or Pd-bulk type catalyst materials, making the former highly competitive anode material for potential application in direct ethanol fuel cell devices. Further work (beyond this introductory examination) will be carried out in order to assess the catalyst's long-time stability in reaction environment along with an intention to derive an optimum Pd loading level in reference to electrocatalytic activity of Pd-activated Ni foam EOR catalyst material.

References

1. Y. Suo, I.M. Hsing, J. Power Sources **196**, 7945 (2011)
2. S.Q. Song, W.J. Zhou, Z.H. Zhou, L.H. Jiang, G.Q. Sun, Q. Xin, V. Leontidis, S. Kontou, P. Tsiakaras, Int. J. Hydrogen Energy **30**, 995 (2005)
3. E.V. Spinace, M. Linardi, A.O. Neto, Electrochem. Commun. **7**, 365 (2005)
4. A. Dutta, S.S. Mahapatra, J. Datta, Int. J. Hydrogen Energy **36**, 14898 (2011)
5. A.M. Sheikh, P.S. Correa, E.L. da Silva, I.D. Savaris, S.C. Amico, C.F. Malfatti, RE&PQJ **11**, 300 (2013)
6. R.M. Modibedi, T. Masombuka, M.K. Mathe, Int. J. Hydrogen. Energy. **36**, 4664 (2011)

7. B. Pierozynski, Int. J. Electrochem. Sci. **7**, 4261 (2012)
8. B. Pierozynski, Int. J. Electrochem. Sci. **7**, 6406 (2012)
9. M. Mitov, E. Chorbadzhiyska, R. Rashkov, Y. Hubenova, Int. J. Hydrogen. Energy **37**, 16522 (2012)
10. M.A. Dominguez-Crespo, A.M. Torres-Huerta, B. Brachetti-Sibaja, A. Flores-Vela, Int. J. Hydrogen. Energy **36**, 135 (2011)
11. R. Solmaz, A. Gundogdu, A. Doner, G. Kardas, Int. J. Hydrogen. Energy **37**, 8917 (2012)
12. F. Bidault, D.J.L. Brett, P.H. Middleton, N. Abson, N.P. Brandon, Int. J. Hydrogen. Energy **34**, 6799 (2009)
13. E. Verlato, S. Cattarin, N. Comisso, A. Gambirasi, M. Musiani, L. Vazquez-Gomez, Electrocatalysis **3**, 48 (2012)
14. D. Wang, J. Liu, Z. Wu, J. Zhang, Y. Su, Z. Liu, C. Xu, Int. J. Electrochem. Sci. **4**, 1672 (2009)
15. S.W. Xie, S. Chen, Z.Q. Liu, C.W. Xu, Int. J. Electrochem. Sci. **6**, 882 (2011)
16. H. Wang, C. Xu, F. Cheng, S. Jiang, Electrochem. Commun. **9**, 1212 (2007)
17. J. Liu, J. Ye, C. Xu, S.P. Jiang, Y. Tong, Electrochem. Commun. **9**, 2334 (2007)
18. B. Pierozynski, Int. J. Electrochem. Sci. **8**, 634 (2013)
19. Y.L. Wang, Y.Q. Zhao, C.L. Xu, D.D. Zhao, M.W. Xu, Z.X. Su, H.L. Li, J. Power Sources **195**, 6496 (2010)
20. J. van Drunen, T.W. Napporn, B. Kokoh, G. Jerkiewicz, J. Electroanal. Chem. **716**, 120 (2014)
21. B. Pierozynski, T. Mikolajczyk, Electrocatalysis (2014). doi:10.1007/s12678-014-0216-z
22. M. Grdeń, M. Alsabet, G. Jerkiewicz, ASC Appl. Mater. Interfaces **4**, 3012 (2012)
23. J. van Drunen, B. Kinkead, M.C.P. Wang, E. Sourty, B.D. Gates, G. Jerkiewicz, ASC Appl. Mater. Interfaces **5**, 6712 (2013)
24. J.R. Macdonald, *Impedance spectroscopy, emphasizing solid materials and systems* (John Wiley, New York, 1987)
25. V. Pecharsky, P. Zavalij, *Fundamentals of powder diffraction and structural characterization of materials*, 2nd edn. (Springer, New York, 2009)
26. X.H. Xia, H.D. Liess, T. Iwasita, J. Electroanal. Chem. **437**, 233 (1997)
27. A.A. Abd-El-Latif, E. Mostafa, S. Huxter, G. Attard, H. Baltruschat, Electrochim. Acta **55**, 7951 (2010)
28. J.F. Gomes, B. Busson, A. Tadjeddine, G. Tremiliosi-Filho, Electrochim. Acta **53**, 6899 (2008)
29. S. Sun, Z. Jusys, R.J. Behm, J. Power Sources **231**, 122 (2013)
30. M. Grdeń, A. Czerwiński, J. Solid State Electrochem. **12**, 375 (2008)
31. A. Lasia, A. Rami, J. Applied Electrochem. **22**, 376 (1992)
32. L. Chen, A. Lasia, J. Electrochem. Soc. **138**, 3321 (1991)
33. J. van Drunen, B.K. Pilapil, Y. Makonnen, D. Beauchemin, B.D. Gates, G. Jerkiewicz, ASC Appl. Mater. Interfaces **6**, 12046 (2014)
34. T. Pajkossy, J. Electroanal. Chem. **364**, 111 (1994)
35. B.E. Conway, B. Pierozynski, J. Electroanal. Chem. **622**, 10 (2008)